

RESEARCH

Open Access



MRI-based radiomics model and nomogram for predicting the outcome of locoregional treatment in patients with hepatocellular carcinoma

Yuxin Wang¹, Zhenhao Liu², Hui Xu¹, Dawei Yang¹, Jiahui Jiang¹, Himeko Asayo¹ and Zhenghan Yang^{1*}

Abstract

Background Prediction of locoregional treatment response is important for further therapeutic strategy in patients with hepatocellular carcinoma. This study aimed to investigate the role of MRI-based radiomics and nomogram for predicting the outcome of locoregional treatment in patients with hepatocellular carcinoma.

Methods The initial postoperative MRI after locoregional treatment in 100 patients with hepatocellular carcinoma was retrospectively analysed. The outcome was evaluated according to mRECIST at 6 months. We delineated the tumour volume of interest on arterial phase, portal venous phase and T2WI. The radiomics features were selected by using the independent sample t test or nonparametric Mann–Whitney U test and the least absolute shrinkage and selection operator. The clinical variables were selected by using univariate analysis and multivariate analysis. The radiomics model and combined model were constructed via multivariate logistic regression analysis. A nomogram was constructed that incorporated the Rad score and selected clinical variables.

Results Fifty patients had an objective response, and fifty patients had a nonresponse. Nine radiomics features in the arterial phase were selected, but none of the portal venous phase or T2WI radiomics features were predictive of the treatment response. The best radiomics model showed an AUC of 0.833. Two clinical variables (hCRP and therapy method) were selected. The AUC of the combined model was 0.867. There was no significant difference in the AUC between the combined model and the best radiomics model ($P=0.573$). Decision curve analysis demonstrated the nomogram has satisfactory predictive value.

Conclusions MRI-based radiomics analysis may serve as a promising and noninvasive tool to predict outcome of locoregional treatment in HCC patients, which will facilitate the individualized follow-up and further therapeutic strategies guidance.

Keywords Hepatocellular carcinoma, Radiomics, Magnetic resonance imaging, Locoregional treatment

*Correspondence:

Zhenghan Yang

yangzhenghan@vip.163.com

¹Department of Radiology, Beijing Friendship Hospital, Capital Medical University, Beijing 100050, China

²Department of Radiology, Affiliated Hospital of Changzhi Institute of Traditional Chinese Medicine, Changzhi 046099, China



© The Author(s) 2023. **Open Access** This article is licensed under a Creative Commons Attribution 4.0 International License, which permits use, sharing, adaptation, distribution and reproduction in any medium or format, as long as you give appropriate credit to the original author(s) and the source, provide a link to the Creative Commons licence, and indicate if changes were made. The images or other third party material in this article are included in the article's Creative Commons licence, unless indicated otherwise in a credit line to the material. If material is not included in the article's Creative Commons licence and your intended use is not permitted by statutory regulation or exceeds the permitted use, you will need to obtain permission directly from the copyright holder. To view a copy of this licence, visit <http://creativecommons.org/licenses/by/4.0/>. The Creative Commons Public Domain Dedication waiver (<http://creativecommons.org/publicdomain/zero/1.0/>) applies to the data made available in this article, unless otherwise stated in a credit line to the data.

Background

Hepatocellular carcinoma (HCC) is the fourth leading cause of death from cancer and there are around 841,080 new cases every year [1, 2], which places a heavy burden on the family economy and social health care. Unfortunately, up to 70% of patients already have advanced HCC at the time of their first visit, so they have lost the opportunity for possible radical treatment such as resection and transplantation [3]. As an important method of locoregional treatment (LRT), transcatheter arterial chemoembolization (TACE) is not only the most common treatment for intermediate stage HCC but is also the first-line therapy across disease stages in China, North America and Europe [4]. TACE even acts as a bridging or downstaging method before resection and transplantation [5]. In addition, according to the Barcelona Clinical Liver Cancer (BCLC) staging system, radiofrequency ablation (RFA) is the first choice for patients with early-stage HCC [6]. However, the highly heterogeneous biological behaviour of tumour cells and liver function of patients with HCC affect the curative effect of LRT. The objective response rate of TACE is about 15–61% and 70–80% of patients who receive TACE will eventually die of tumour progression [7–10]. Patients who respond poorly to LRT need timely conversion to systemic therapy, such as sorafenib and targeted kinase inhibitor [11–13]. Therefore, it is essential to predict the outcome of LRT.

Several indicators have been shown to be related to HCC prognosis after LRT, including clinical characteristics such as alpha fetoprotein and imaging features such as tumour size, tumour numbers, the presence of nonsmoothed tumour margins, hypoattenuating halos and internal arteries [14–17]. Furthermore, several studies have shown that radiomics models with or without clinical factors can predict initial treatment response or long-term survival after LRT in HCC patients [18–22]. Nevertheless, most of the research used preoperative images which cannot provide information on the sensitivity of tumour cells to LRT. The response to initial treatment was likely influenced by operator experience. Recently, Godefroy A et al. reported that postoperative arterial phase radiomics features could predict early treatment response to ⁹⁰yttrium transarterial radioembolization in patients with HCC [23]. Several studies have shown that texture analysis and radiomics of postoperative CT images can be used to evaluate local recurrence and tumour progression after ablation [24, 25]. However, there has been no radiomics model based on initial postoperative MRI for predicting treatment response to LRT.

The aim of this study was to investigate the role of MRI-based radiomics and nomogram for predicting the outcome of LRT at 6 months, which may contribute

to guiding individualized treatment and follow-up in patients with HCC.

Patients and methods

Patients

This study was approved by the Institutional Review Board of our hospital and the requirement for informed consent was waived. We retrospectively collected patients who underwent LRT in our hospital between January 2015 and April 2022. Informed consent requirement was waived due to the retrospective nature of the study. The inclusion criteria were (1) presence of HCC diagnosed by pathology or typical imaging findings according to the guidelines of the American Association for the Study of Liver Disease (AASLD), (2) initial treatment was TACE or RFA, (3) aged > 18 years, (4) MRI within 2 months after initial LRT, and (5) availability of mRECIST at 6 months. The exclusion criteria were (1) previous treatments, including liver resection and transplantation (n=5), (2) diffuse or infiltrative lesions (n=9), and (3) incomplete MRI sequences or poor image quality (n=3). Finally, 100 patients were included in the study and were randomly divided into the training cohort (n=70) and the validation cohort (n=30) at a ratio of 7:3 (Fig. 1).

Postoperative clinical characteristics of the enrolled patients, including sex, age, Barcelona Clinic Liver Cancer (BCLC) stage, history of chronic liver disease, alpha-fetoprotein (AFP), aspartate aminotransferase (AST), alanine aminotransferase (ALT), alkaline phosphatase (ALP), gamma-glutamyltranspeptidase (GGT), total bilirubin (TBIL), indirect bilirubin (IBIL), direct bilirubin (DBIL), and high-sensitivity C-reactive protein (hCRP), were collected.

Locoregional treatment methods

TACE was performed under the guidance of digital subtraction angiography (GE Innova 3100) using the Seldinger technique. The femoral artery was punctured at the groin area and a 2.2–2.4 F microcatheter (Asahi Intecc Co. Ltd, Japan) was inserted into the feeding hepatic artery, then chemoembolization was performed. This emulsion was created using 10 ml of lipiodol (Alicon, Hanzhou, China) and 10ml of chemotherapeutic agent (with 50 mg of doxorubicin). The volume of chemoembolic emulsion injected depended on patient factors and tumor size. Following this injection, 100–300 µm gelatin sponge particles was administered to achieve the embolization end point. Percutaneous RFA was performed under the guidance of CT (GE Revolution). Two RFA systems, Rita Starburst T Flex/talon electrode (RITA Medical Systems, Mountain View, Calif., USA), and CELON ProSurge (Olympus Winter & Ibe GmbH, Hamburg, Germany) with a deployment 2–5 cm determined by type of generator model, which were equipped with internal

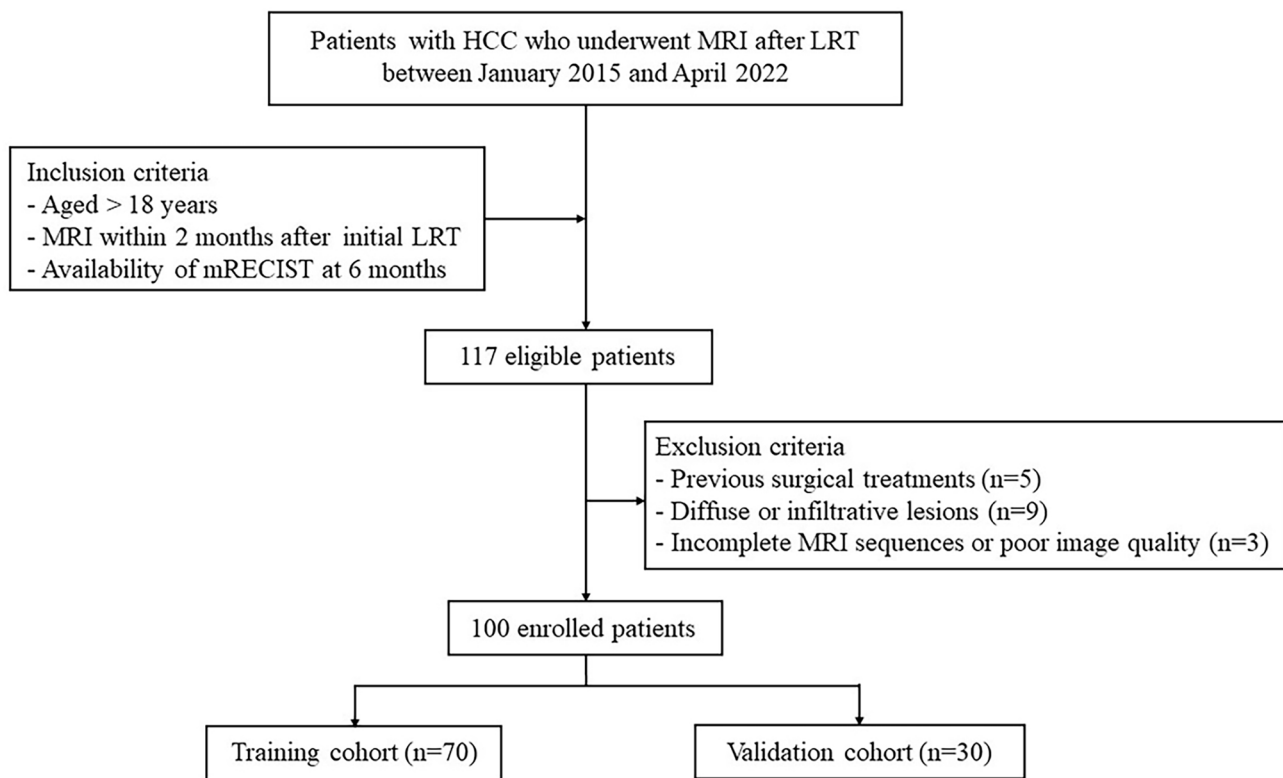


Fig. 1 Flowchart of patient selection

Table 1 MRI Scanning Parameters

| | T2WI | Dynamic multi-phase contrast-enhanced T1WI |
|----------------------|------------------------|--|
| Breath | Respiratory triggering | Hold breath |
| Fat suppression | Yes | Yes |
| TR (ms) | 2–3 respiratory cycles | 3.4–4.1 |
| TE (ms) | 85 | 1.15–1.91 |
| Flip angle (°) | 150 | 15 |
| Matrix | 288 × 224 | 288 × 172–320 × 216 |
| FOV (mm) | 380–420 | 380–420 |
| Slice thickness (mm) | 6–8 | 3–4 |

liquid circulation (saline solution) keeping surface temperature. The generator model selection and electrode shaft distribution were depended on the size, location and adjacent structure of the tumor. The assistance of multiplanar reformation ensured that the tip of the electrode shaft was inside or at the center of the tumor covered in expandable needles with at least 5–10 mm safety margin. Ablation-related parameters were set as per manufacturer's instructions regarding tumor-related characteristics.

Image acquisition

MRI examinations were obtained within 2 months after initial LRT and performed from standard institutional liver MRI protocols using 1.5-T and 3.0-T MRI scanners, including Siemens (Prisma, Magnetom), GE Healthcare (750w Discovery, HDi Signa) and Philips (Ingenia, dStream) systems. The following sequences were used: T2WI, dynamic multiphase contrast-enhanced T1WI. Detailed scanning parameters are described in Table 1. The images in the arterial phase and portal venous phase were acquired at 15–20 s and 60–70 s after the initiation of an intravenous injection of gadopentetate dimeglumine (Magnevist, Bayer Schering Pharma AG) at a dosage of 0.1 mmol/kg and a rate of 2.0 ml/s followed by a normal saline flush.

Treatment response assessment

The primary outcome was the tumour response of the target lesion at 6 months, according to mRECIST. The responses were classified as follows: (i) complete response was the disappearance of any intratumoural arterial enhancement in the target lesion; (ii) partial response was at least a 30% decrease in the sum of the longest viable tumour diameters of the target lesion; (iii) stable disease was any patient that showed neither a sufficient decrease to qualify for partial response nor a sufficient increase to qualify for progressive disease; and

(iv) progressive disease was at least a 20% increase in the sum of the longest viable tumour diameters of the target lesion. For T1-weighted image hyperintense lesions, subtraction images were used to assist in the evaluation of treatment response. Objective response (OR) included complete response and partial response, whereas non-response (NR) included stable disease and progressive disease. The tumour response was evaluated by two radiologists (each with >20 years of experience in hepatic imaging). The disagreements between the two radiologists were resolved through consultation.

Radiomics analysis

To reduce the potential impact among different vendors, scanners and scanning parameters, all MRI sequences were normalized using the Z score. N4 bias correction was performed to normalize nonuniform intensity. Then, the tumour volume of interest (VOI) was manually delineated slice-by-slice on arterial phase, portal venous phase and T2-weighted images (T2WI) by a radiologist with 5 years of experience in abdominal imaging using 3D Slicer V5.0.3 (<https://www.slicer.org/>) software. The VOIs were checked and adjusted by a senior radiologist with 20 years of experience in abdominal imaging. Next, the VOIs were resampled into voxels of 1×1×1 mm. A total of 851 radiomics features were finally extracted from each VOI using the 3D slicer. The extracted radiomics features were divided into eight categories: 18 first-order statistics features, 14 shape-based features, 24 grey level cooccurrence matrix (GLCM) features, 14 grey level

dependence matrix (GLDM) features, 16 grey level size zone matrix (GLSZM) features, 16 grey level run length matrix (GLRLM) features, 5 neighbouring grey tone difference matrix (NGTDM) features, and 744 wavelet transformed features.

The significantly different radiomics features between OR and NR in the training cohort were selected by using the independent sample t test or nonparametric Mann-Whitney U test. Then, least absolute shrinkage and selection operator (LASSO) with penalty parameter tuning conducted by 5-fold cross-validation was further performed to identify the most valuable features. To avoid unit limits on the data of radiomics features, Z score normalization was used in the training cohort and the validation cohort. The radiomics models were constructed using the selected features via multivariate logistic regression analysis. The radiomics score (Rad score) was a linear combination cluster of the selected feature multiplied by the corresponding LASSO coefficient.

The significantly different clinical variables between OR and NR in the training cohort were selected by using univariate analysis and multivariate analysis. The combined model was constructed using the above selected radiomics features and clinical variables via a multivariate logistic regression algorithm. Then, a nomogram was constructed incorporating the Rad score and selected clinical variables. The radiomics workflow is presented in Fig. 2.

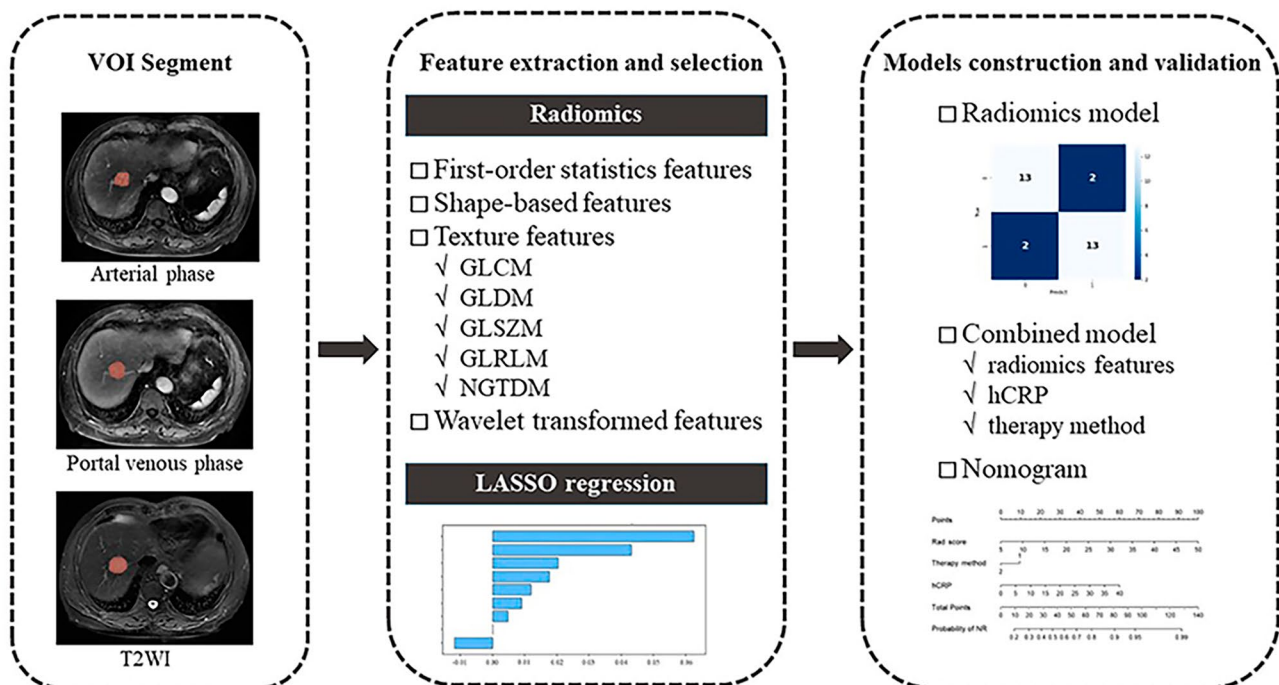
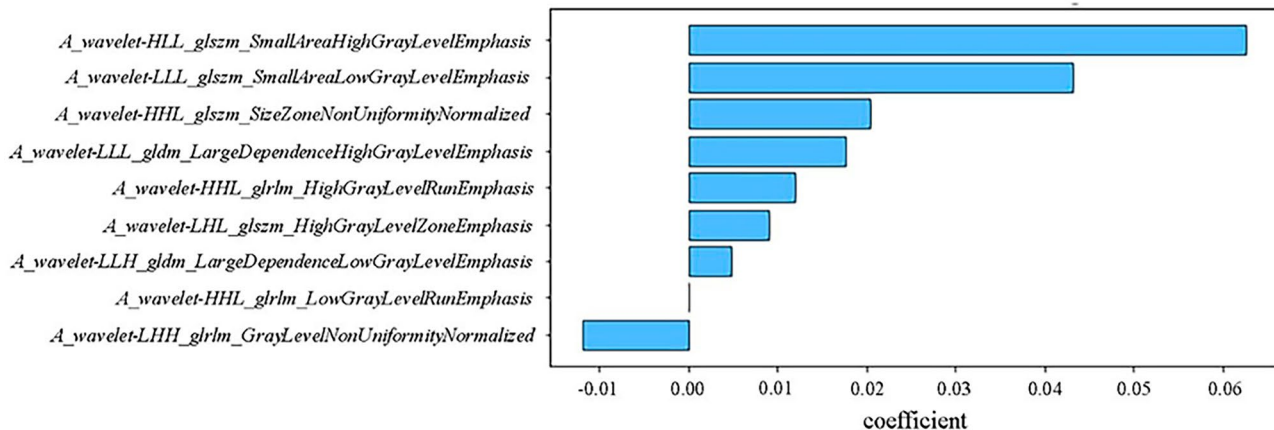


Fig. 2 Flowchart of radiomics model and nomogram construction

Table 2 Patient clinical characteristics

| | Training cohort (n=70) | Validation cohort (n=30) | Univariate analysis in the training cohort | | | Multivariate analysis in the training cohort |
|---------------------------------------|------------------------|--------------------------|--|----------------------|--------------|--|
| | | | OR (n=35) | NR (n=35) | P value | P value |
| Treatment response (OR:NR) | 35:35 | 15:15 | / | / | / | / |
| Age | 63.2±11.8 | 61.6±9.3 | 63.3±11.7 | 63.0±12.1 | 0.895 | |
| Sex (M:F) | 48:22 | 25:5 | 21:14 | 27:8 | 0.126 | |
| AFP(>15ng/ml) | 26 | 7 | 10 | 16 | 0.141 | |
| hCRP(mg/L) | 2.18 (0.78~10.45) | 2.14 (0.94~7.21) | 1.85 (0.76~5.84) | 4.14 (0.96~21.32) | 0.012 | 0.033 |
| ALT(>50U/L) | 10 | 3 | 5 | 5 | 1.000 | |
| AST(>40U/L) | 19 | 7 | 9 | 10 | 0.788 | |
| GGT(>60U/L) | 25 | 10 | 10 | 15 | 0.215 | |
| ALP(>125U/L) | 25 | 10 | 10 | 15 | 0.215 | |
| TBIL(>17.1umol/L) | 35 | 21 | 14 | 21 | 0.097 | |
| DBIL(>6.84umol/L) | 21 | 10 | 7 | 14 | 0.072 | |
| IBIL(>12umol/L) | 39 | 21 | 17 | 22 | 0.231 | |
| With history of chronic liver disease | 61 | 27 | 31 | 30 | 0.722 | |
| BCLC (A:B) | 55:15 | 23:7 | 31:4 | 24:11 | 0.049 | |
| Therapy method (TACE:RFA) | 46:24 | 23:7 | 18:17 | 28:7 | 0.014 | 0.048 |

**Fig. 3** The coefficients of the selected radiomics features

Statistical analysis

Python 3.9.12 software was used to select radiomics features and construct models. The predictive efficiency of the radiomics model and combined model was quantified by the area under the receiver operating characteristic (ROC) curve (AUC) in the validation cohort. Comparisons between the AUCs of the radiomics model and combined model were performed using Delong's test. Calibration curves and the Hosmer–Lemeshow test were used to evaluate the predictive efficiency of the nomogram. Continuous variables between the training cohort and the validation cohort were compared using Student's t test or the Mann–Whitney U test, and categorical variables were compared using the chi-squared

test or Fisher's exact test. $P < 0.05$ was considered to indicate statistically significant differences.

Results

Patient characteristics

In this study, 50 patients had OR, and the other 50 patients had NR. The clinical characteristics are shown in Table 2. The clinical characteristics between the training cohort and the validation cohort were balanced for there was no significant difference between the two groups.

Radiomics model

Nine radiomics features in the arterial phase were selected after LASSO, and the coefficients are presented in Fig. 3. None of the portal venous phase or T2WI

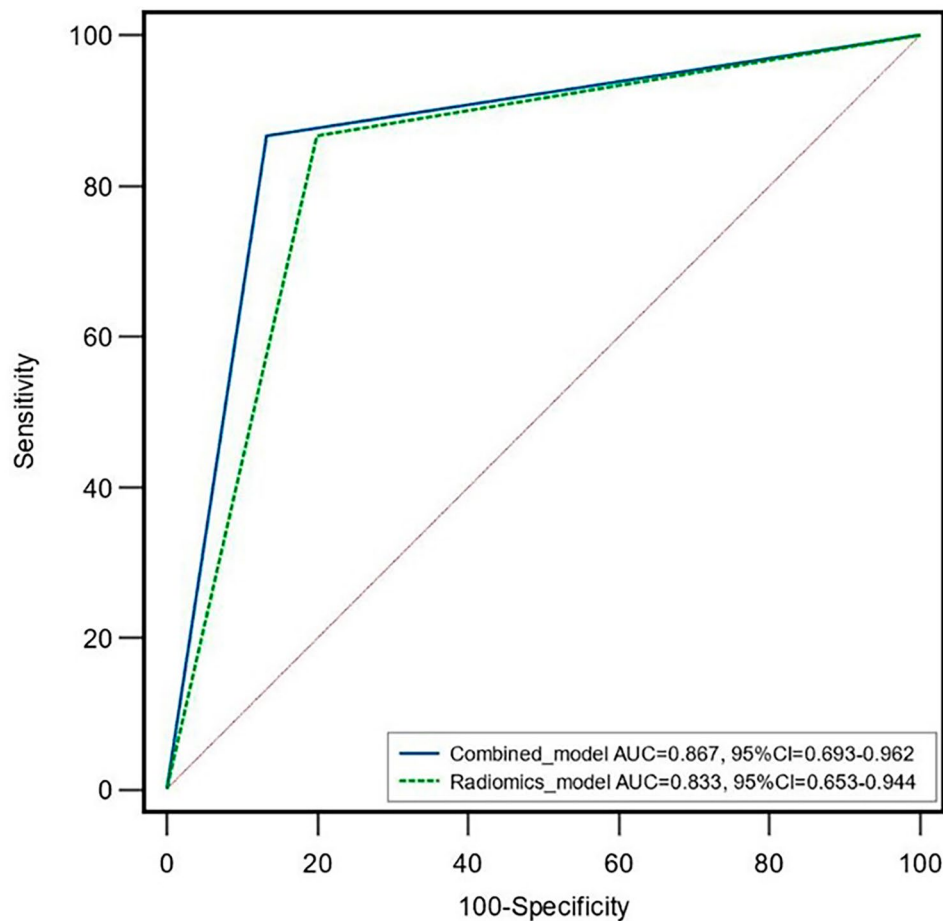


Fig. 4 ROC curves of the radiomics model and combined model

Table 3 Distinguishing efficiency of the two models

| | Sensitivity | Specificity | Accuracy | AUC |
|----------------------|-------------|-------------|----------|-------|
| Best radiomics model | 0.87 | 0.80 | 0.83 | 0.833 |
| Combined model | 0.87 | 0.87 | 0.87 | 0.867 |

radiomics features were predictive of the treatment response. Nine radiomics models were built by removing the radiomics features in sequence according to the coefficients. The best radiomics model with the first five radiomics features showed the highest AUC of 0.833 (95% CI, 0.653–0.9440 in the validation cohort).

Combined model

Two clinical variables (hCRP and therapy method) were selected through the univariate analysis and multivariate analysis (Table 2). A combined model was built incorporating the best five radiomics features and the two clinical variables. The AUC of the combined model was 0.867 (95% CI, 0.693–0.962) in the validation cohort. However, there was no significant difference in the AUC between the combined model and the best radiomics model

($P=0.573$), as shown in Fig. 4. The distinguishing efficiency of the two models is shown in Table 3.

Nomogram

The nomogram was constructed with the Rad score and selected two clinical variables to individually predict tumour response (Fig. 5). The calibration curves demonstrated good agreement between the prediction and the observation in both cohorts (Fig. 6). The Hosmer–Lemeshow test showed nonsignificant result suggesting a satisfying fit of the nomogram.

Discussion

The present study constructed a radiomics model and a combined model for predicting the outcome of LRT at 6 months in HCC patients, and the models had AUCs of 0.833 and 0.867, respectively, in the validation cohort. Also, a nomogram was established based on Rad scores and clinical variables and could stratify patients into OR and NR groups. To the best of our knowledge, this is the first study using a radiomics model based on initial

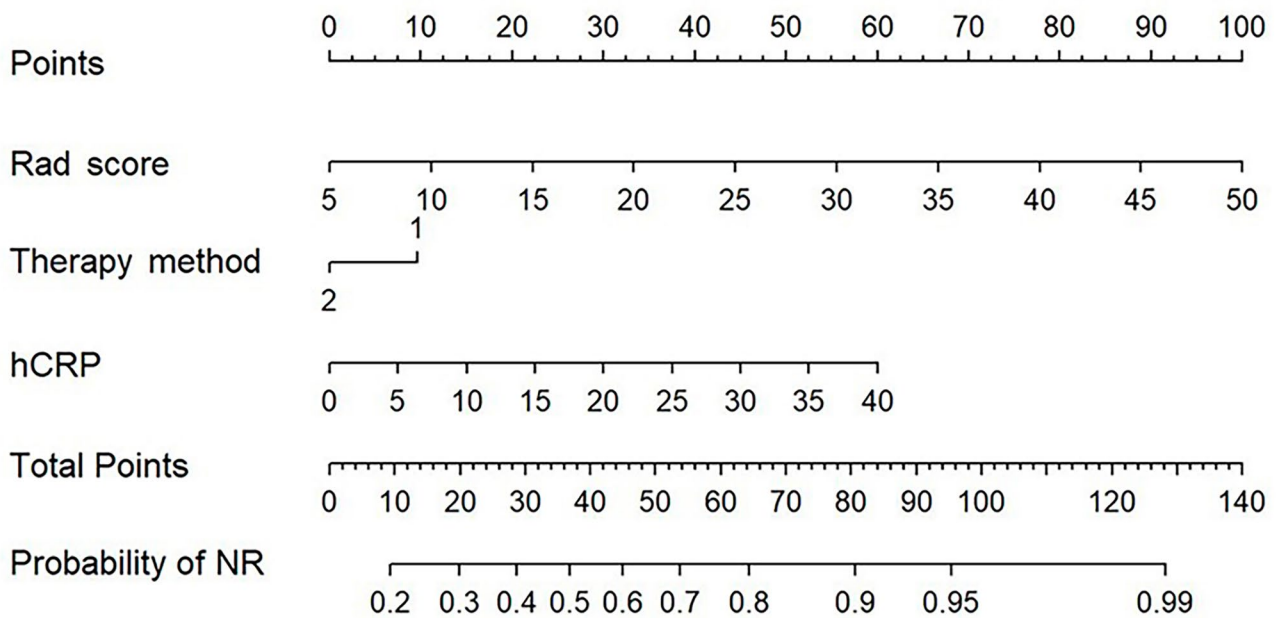


Fig. 5 Nomogram based on Rad score, therapy method and hCRP. The probability of NR for each patient is marked on the axis

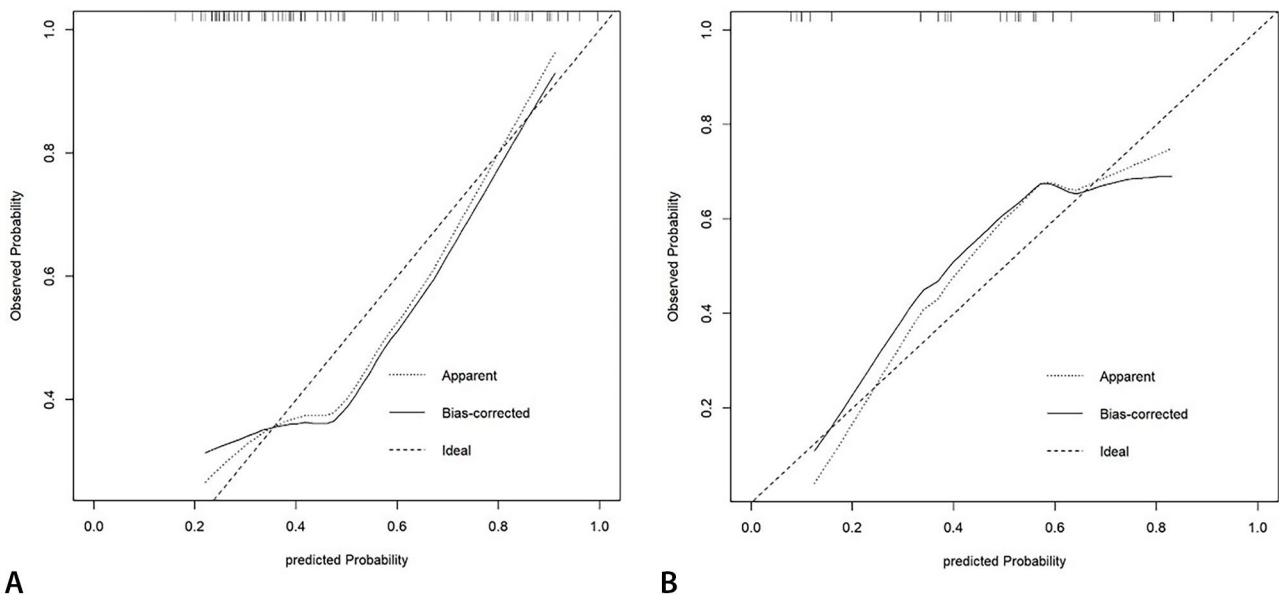


Fig. 6 The calibration curves in the training cohort (A) and the validation cohort (B). The diagonal dotted line represents the ideal evaluation, while the solid lines and dashed lines represent the performance of the corrected and apparent bias, respectively. The prediction solid line is close to the ideal dotted line, meaning that the model has good prediction accuracy

postoperative MRI to predict the treatment response of HCC patients undergoing LRT.

Previous studies have shown that radiomics models with or without clinical factors had good performance in predicting the first TACE response in patients with HCC (AUC 0.815-0.900) [26–28]. We assessed the treatment response at 6 months, which possessed more clinical value than that after the first treatment. Recent

report used MRI radiomics nomogram to predict recurrence after ablation at 1, 2, and 3 years in HCC patients, the AUCs of which (0.72, 0.61 and 0.64) were lower than our study (0.867) [29]. Moreover, most published studies used CT-based radiomics [21, 22, 24, 26–28, 30], but MRI is known to have higher soft-tissue contrast than CT and is more commonly used in treated HCC viability evaluation. Based on the reports that postoperative

CT and MRI were of predictive value for outcome of LRT [23–25], our study used initial postoperative MRI.

The patients in our study at BCLC B or A stage received TACE or RFA, reflecting the real phenomenon in the clinical setting. There was no significant difference in BCLC stage between OR and NR in the training cohort after the multivariate analysis. Therapy method showed significant difference and was put into combined model. Nevertheless, the radiomics model without regard to the therapy method showed satisfactory predictive ability, and the AUC of the combined model was higher than that of the radiomics model without significant difference. Our study enrolled patients receiving TACE or RFA, which attached the model wider clinical application.

Our study used MRI-based radiomics and performed normalization to correct the scanner and individual effect. In addition, no radiomics feature in the portal venous phase and T2WI was selected after LASSO, consistent with clinical experience that viability evaluation mainly relies on the arterial phase; thus, we established the radiomics model based on only the arterial phase, which is simple and convenient in clinical practice. A previous study also indicated that only postoperative arterial phase radiomics features were predictors for treatment response in patients with HCC [24] and supported our findings. We obtained the best radiomics model using the first five of the nine selected radiomics features, consistent with the literature that the number of selected radiomics features should be less than 10% of the total number of positive cases [31].

To improve general applicability, we constructed a nomogram based on the Rad score, therapy method and hCRP. Calibration curves demonstrated favourable prediction performance of our nomogram. Several studies have shown that hCRP was marker of poor prognosis in patients with HCC [32, 33]. However, unlike previous literature, we found that AFP had no relationship with treatment response at 6 months. This may be because AFP in our study was collected after initial treatment.

This study has several limitations. First, this was a single-centre retrospective study, the sample size of patients was relatively small, and the study results were without external validation. A much larger database of prospective studies will be collected from more centres in the future. Second, we used MRI machines with different Tesla intensity (1.5 vs. 3T), which could reduce the accuracy of our model. Third, delineating the VOIs mostly depended on the radiologists' experience, and the manual method required considerable time and energy. Future studies could develop an automatic segmentation model for focal liver lesions to minimize discrepancies. Last, the biological mechanisms resulting in these radiomics features are still unknown. Multiomics, including radiomics,

genetics and proteomics, will become the focus of future research.

Conclusion

In conclusion, radiomics features derived from initial postoperative MRI may be potential biomarkers for predicting tumour response to LRT at 6 months. The nomogram with the Rad score and clinical variables demonstrated favourable prediction performance and general applicability which may aid in further treatment planning in patients with HCC.

Abbreviations

| | |
|-----------|--|
| HCC | Hepatocellular carcinoma |
| LRT | Locoregional treatment |
| TACE | Transcatheter arterial chemoembolization |
| RFA | Radiofrequency ablation |
| OR | Objective response |
| NR | Nonresponse |
| Rad score | Radiomics score |

Acknowledgements

Not applicable.

Authors' contribution

Yuxin Wang designed this study and wrote the main manuscript. Zhenhao Liu, Hui Xu and Dawei Yang contributed to the data analysis and manuscript writing. Jiahui Jiang and Himeko Asayo were involved in performing data collection. Zhenghan Yang was responsible for the study coordination. All authors reviewed the manuscript.

Funding

This study was supported by National Natural Science Foundation of China [grant numbers 62171298]. The funding body played no role in the design of the study and collection, analysis, interpretation of data, and in writing the manuscript.

Data Availability

The datasets used and analysed in the current study are available from the corresponding author on reasonable request.

Declarations

Ethics approval and consent to participate

The study was approved by the ethics committee of Beijing Friendship Hospital, Capital Medical University. All methods were carried out in accordance with relevant guidelines and regulations. The need for informed consent was waived by the ethics committee of Beijing Friendship Hospital, Capital Medical University, because of the retrospective nature of the study.

Consent for publication

Not applicable.

Competing interests

The authors declare that they have no competing interests.

Received: 2 April 2023 / Accepted: 23 May 2023

Published online: 30 May 2023

References

1. Villanueva A. Hepatocellular carcinoma. *N Engl J Med*. 2019;380:1450–62.
2. Bray F, Ferlay J, Soerjomataram I, et al. Global cancer statistics 2018: GLOBOCAN estimates of incidence and mortality worldwide for 36 cancers in 185 countries. *CA Cancer J Clin*. 2018;68:394–424.

3. European Association for the Study of the Liver. EASL Clinical Practice Guidelines: management of hepatocellular carcinoma. *J Hepatol*. 2018;69:182–236.
4. Park J, Chen M, Colombo M, et al. Global patterns of hepatocellular carcinoma management from diagnosis to death: the BRIDGE Study. *Liver Int*. 2015;35:2155–66.
5. Heimbach JK, Kulik LM, Finn RS, et al. AASLD guidelines for the treatment of hepatocellular carcinoma. *Hepatology*. 2018;67:358–80.
6. Zhou J, Sun HC, Wang Z, et al. Guidelines for diagnosis and treatment of hepatocellular carcinoma (2019 edition). *Liver Cancer*. 2020;9:682–720.
7. Shin SW. The current practice of transarterial chemoembolization for the treatment of hepatocellular carcinoma. *Korean J Radiol*. 2009;10:425–34.
8. Guan YS, He Q, Wang MQ. Transcatheter arterial chemoembolization: history for more than 30 years. *ISRN Gastroenterol*. 2012.
9. Raoul JL, Sangro B, Forner A, et al. Evolving strategies for the management of intermediate-stage hepatocellular carcinoma: available evidence and expert opinion on the use of transarterial chemoembolization. *Cancer Treat Rev*. 2011;37:212–20.
10. Boulin M, Ciboulet A, Guiu B, et al. Randomised controlled trial of lipiodol transarterial chemoembolisation with or without amiodarone for unresectable hepatocellular carcinoma. *Dig Liver Dis*. 2011;43:905–11.
11. Lin H, Lin L, Wang G, et al. Label-free classification of hepatocellular carcinoma grading using second harmonic generation microscopy. *Biomed Opt Express*. 2018;9:3783–93.
12. Ogasawara S, Chiba T, Ooka Y, et al. Efficacy of sorafenib in intermediate-stage hepatocellular carcinoma patients refractory to transarterial chemoembolization. *Oncology*. 2014;87:330–41.
13. Arizumi T, Ueshima K, Minami T, et al. Effectiveness of sorafenib in patients with transcatheter arterial chemoembolization (TACE) refractory and intermediate-stage hepatocellular carcinoma. *Liver Cancer*. 2015;4:253–62.
14. Li ZW, Ren AH, Yang DW, et al. Preoperatively predicting early response of HCC to TACE using clinical indicators and MRI features. *BMC Med Imaging*. 2022;22:176.
15. Tateishi R, Okanou T, Fujiwara N, et al. Clinical characteristics, treatment, and prognosis of non-B, non-C hepatocellular carcinoma: a large retrospective multicenter cohort study. *J Gastroenterol*. 2015;50:350–60.
16. Tandon P, Garcia-Tsao G. Prognostic indicators in hepatocellular carcinoma: a systematic review of 72 studies. *Liver Int*. 2009;29:502–10.
17. Lauwers GY, Terris B, Balis UJ, International Cooperative Study Group on Hepatocellular Carcinoma, et al. Prognostic histologic indicators of curatively resected hepatocellular carcinomas: a multi-institutional analysis of 425 patients with definition of a histologic prognostic index. *Am J Surg Pathol*. 2002;26:25–34.
18. Kong C, Zhao Z, Chen W, et al. Prediction of tumor response via a pretreatment MRI radiomics-based nomogram in HCC treated with TACE. *Eur Radiol*. 2021;31:7500–11.
19. Zhao Y, Wang N, Wu J, et al. Radiomics analysis based on contrast-enhanced MRI for prediction of therapeutic response to transarterial chemoembolization in hepatocellular carcinoma. *Front Oncol*. 2021;11:582788.
20. Sun Y, Bai H, Xia W, et al. Predicting the outcome of transcatheter arterial embolization therapy for unresectable hepatocellular carcinoma based on radiomics of preoperative multiparameter MRI. *J Magn Reson Imaging*. 2020;52:1083–90.
21. Kim J, Choi SJ, Lee SH, et al. Predicting Survival using pretreatment CT for patients with hepatocellular carcinoma treated with transarterial chemoembolization: comparison of models using Radiomics. *AJR Am J Roentgenol*. 2018;211:1026–34.
22. Dai Y, Jiang H, Feng ST, et al. Noninvasive imaging evaluation based on computed tomography of the efficacy of initial transarterial chemoembolization to predict outcome in patients with hepatocellular carcinoma. *J Hepatocell Carcinoma*. 2022;9:273–88.
23. Aujay G, Etchegaray C, Blanc J, et al. Comparison of MRI-based response criteria and radiomics for the prediction of early response to transarterial radioembolization in patients with hepatocellular carcinoma. *Diagn Interv Imaging*. 2022;107:360–6.
24. Beleu A, Autelitano D, Geraci L, et al. Radiofrequency ablation of hepatocellular carcinoma: CT texture analysis of the ablated area to predict local recurrence. *Eur J Radiol*. 2022;150:110250.
25. Staal FCR, Taghavi M, Reijnd DJ, et al. Predicting local tumour progression after ablation for colorectal liver metastases: CT-based radiomics of the ablation zone. *Eur J Radiol*. 2021;141:109773.
26. Chen M, Cao J, Hu J, et al. Clinical-radiomic analysis for pretreatment prediction of objective response to first transarterial chemoembolization in hepatocellular carcinoma. *Liver Cancer*. 2021;10:38–51.
27. Peng J, Kang S, Ning Z, et al. Residual convolutional neural network for predicting response of transarterial chemoembolization in hepatocellular carcinoma from CT imaging. *Eur Radiol*. 2020;30:413–24.
28. Guo Z, Zhong N, Xu X, et al. Prediction of hepatocellular carcinoma response to transcatheter arterial chemoembolization: a real-world study based on non-contrast computed tomography radiomics and general image features. *J Hepatocell Carcinoma*. 2021;8:773–82.
29. Yang X, Yuan C, Zhan Y, et al. Predicting hepatocellular carcinoma early recurrence after ablation based on magnetic resonance imaging radiomics nomogram. *Med (Baltim)*. 2022;101:e32584.
30. Bai H, Meng S, Xiong C, et al. Preoperative CECT-based Radiomic signature for Predicting the response of Transarterial Chemoembolization (TACE) therapy in Hepatocellular Carcinoma. *Cardiovasc Intervent Radiol*. 2022;45:1524–33.
31. Jiang L, Wang S, Ai Z, et al. Development and external validation of a stability machine learning model to identify wake-up stroke onset time from MRI. *Eur Radiol*. 2022;32:3661–9.
32. Li Z, Xue T, Chen X. Predictive values of serum VEGF and CRP levels combined with contrast enhanced MRI in hepatocellular carcinoma patients after TACE. *Am J Cancer Res*. 2016;6:2375–85.
33. Nagaoka S, Yoshida T, Akiyoshi J, et al. Serum C-reactive protein levels predict survival in hepatocellular carcinoma. *Liver Int*. 2007;27:1091–7.

Publisher's Note

Springer Nature remains neutral with regard to jurisdictional claims in published maps and institutional affiliations.